J|A|C|S
ARTICLES
Published on Web 08/24/2005

Metal versus Ligand Alkylation in the Reactivity of the (Bis-iminopyridinato)Fe Catalyst

Jennifer Scott,[†] Sandro Gambarotta,*[,†] Ilia Korobkov,[†] and Peter H. M. Budzelaar*[,‡]

Contribution from the Department of Chemistry, University of Ottawa, Ottawa, Ontario K1N 6N5, Canada, and Department of Inorganic Chemistry, Radboud University Nijmegen, Toernooiveld 1, 6525 ED Nijmegen, The Netherlands

Received June 23, 2005; E-mail: sgambaro@science.uottawa.ca; budzelaa@cc.umanitoba.ca

Abstract: The alkylation of the Brookhart−Gibson {2,6-[2,6-(*i*-Pr)$_2$PhN═C(CH$_3$)]$_2$(C$_5$H$_3$N)} FeCl$_2$ precatalyst with 2 equiv of LiCH$_2$Si(CH$_3$)$_3$ led to the isolation of several catalytically very active products depending on the reaction conditions. The expected dialkylated species {2,6-[2,6-(*i*-Pr)$_2$PhN═C(CH$_3$)]$_2$}(C$_5$H$_3$N)Fe(CH$_2$SiMe$_3$)$_2$ (**2**) was indeed the major component of the reaction mixture. However, other species in which alkylation occurred at the pyridine ring *ortho* position, {2,6-[2,6-(*i*-Pr)$_2$PhN═C(CH$_3$)]$_2$-2-CH$_2$SiMe$_3$}(C$_5$H$_3$N)Fe(CH$_2$SiMe$_3$) (**1**), and at the imine C atom, {2-[2,6-(*i*-Pr)$_2$PhN═C(CH$_3$)]-6-[2,6-(*i*-Pr)$_2$PhNC(CH$_3$)(CH$_2$ SiMe$_3$)](C$_5$H$_3$N)}Fe(CH$_2$SiMe$_3$) (**3**)**,** have also been isolated and fully characterized. In addition, deprotonation of the methyl-imino functions and formation of a new divalent Fe catalyst {[2,6-[2,6-(*i*-Pr)$_2$PhN−C═(CH$_2$)]$_2$(C$_5$H$_3$N)}Fe(μ-Cl)Li(THF)$_3$ (**4**) also occurred depending on the reaction conditions. In turn, the formation of **4** might trigger the reductive coupling of two units through the methyl-carbon wings. This process resulted in the one-electron reduction of the metal center, affording a dinuclear Fe(I) alkyl catalyst {[{[2,6-(*i*-Pr)$_2$C$_6$H$_5$]N═C(CH$_3$)}(C$_5$H$_3$N){[2,6-(*i*-Pr)$_2$C$_6$H$_5$]N═CCH$_2$}Fe(CH$_2$SiMe$_3$)]}$_2$ (**5**). Different from other metal derivatives, complex **5** could not be prepared from the monodeprotonated version of the ligand. Its reaction with a mixture of FeCl$_2$ and RLi afforded instead [{2,6-[2,6-(*i*-Pr)$_2$PhN−C═(CH$_2$)]$_2$(C$_5$H$_3$N)}FeCH$_2$Si(CH$_3$)$_3$][Li(THF)$_4$] (**6**) which is also catalytically active. All of these high-spin species have been shown to have high catalytic activity for olefin polymerization, producing polymers of two distinct natures, depending on the formal oxidation state of the metal center.

Introduction

The tremendous activity displayed by diimine complexes of late transition metals as olefin polymerization catalysts has increasingly attracted interest since the initial discoveries by Brookhart and Gibson[1] and fueled research aimed at understanding these fascinating systems. The bis-iminopyridine complexes, and the Fe derivative {2,6-[2,6-(*i*-Pr)$_2$PhN═C(CH$_3$)]$_2$-(C$_5$H$_3$ N)}FeCl$_2$ in particular, are especially prominent in this family of Ziegler−Natta catalysts, given their outstanding activity that rivals even that of the early metal-based commercial catalysts. The three key issues at the basis of the exceptional catalytic performance of these systems, which still remain not well understood, are (1) the role played by the ligand system, (2) the oxidation state and electronic configuration of the metal in the catalytically active species, and (3) the stability of the M−C bond.

Recent work in the chemistry of vanadium,[2] chromium,[3] manganese,[3,4] cobalt,[5] and lanthanides[6] has clearly pointed toward a nonanticipated ability of the diimine ligand to be involved in the reactivity of the M−C bond. The ligand is definitely noninnocent and has been shown to engage in a series of transformations. These involve alkylation at any position of the pyridine ring,[2,3] including the N atom,[7] deprotonation of the methyl sidearms,[3,7b,8,9] alkylation of the imine functions,[10] and even dimerization via either C−C bond formation through the deprotonated alkyl substituents[3,5,6] or pyridine ring cycloaddition.[3] Some of these processes can be reversed and may or may not involve redox of the metal center.

The second point concerns the actual oxidation state and electronic configuration of the metal center. The bis-imino-

[†] University of Ottawa.
[‡] Radboud University of Nijmegen.

(1) (a) Johnson, L. K.; Killian, C. M.; Brookhart, M. S. *J. Am. Chem. Soc.* **1995**, *117*, 6414. (b) Killian, C. M.; Tempel, D. J.; Johnson, L. K.; Brookhart, M. S. *J. Am. Chem. Soc.* **1996**, *118*, 11664. (c) Small, B. L.; Brookhart, M.; Bennett, A. M. A. *J. Am. Chem. Soc.* **1998**, *120*, 4049. (d) Britovsek, G. J. P.; Gibson, V. C.; Kimberley, B. S.; Maddox, P. J.; McTavish, S. J.; Solan, G. A.; White, A. J. P.; Williams, D. J. *Chem. Commun*. **1998**, 849.
(2) Reardon, D.; Conan, F.; Gambarotta, S.; Yap, G. P. A.; Wang, Q. *J. Am. Chem. Soc.* **1999**, *121*, 9318.
(3) Sugiyama, H.; Aharonian, G.; Gambarotta, S.; Yap, G. P. A.; Budzelaar, P. H. M. *J. Am. Chem. Soc.* **2002**, *124*, 12268.
(4) Reardon, D.; Aharonian, G.; Gambarotta, S.; Yap, G. P. A. *Organometallics* **2002**, *21*, 786.
(5) Scott, J.; Gambarotta, S.; Korobkov, I. *Can. J. Chem.* **2005**, *83*, 279.
(6) Sugiyama, H.; Korobkov, I.; Gambarotta, S.; Moeller, A.; Budzelaar, P. H. M. *Inorg. Chem.* **2004**, *43*, 5771.
(7) (a) Clentsmith, G. K. B.; Gibson, V. C.; Hitchcock, P. B.; Kimberley, B. S.; Rees, C. W. *Chem. Commun.* **2002**, 1498. (b) Khorobkov, I.; Gambarotta, S.; Yap, G. P. A. *Organometallics* **2002**, *21*, 3088. (c) Blackmore, I. J.; Gibson, V. C.; Hitchcock, P. B.; Rees, C. W.; Williams, D. J.; White, A. J. P. *J. Am. Chem. Soc.* **2005**, *127*, 6012.
(8) Enright, D.; Gambarotta, S.; Yap, G. P. A.; Budzelaar, P. H. M. *Angew. Chem., Int. Ed.* **2002**, *41*, 3873.
(9) Sugiyama, H.; Gambarotta, S.; Yap, G. P. A.; Wilson, D. R.; Thiele, S. K.-H. *Organometallics* **2004**, *23*, 5054.
(10) Bruce, M.; Gibson, V. C.; Redshaw, C.; Solan, G. A.; White, A. J. P.; Williams, D. J. *Chem. Commun.* **1998**, 2523.

pyridine ligand system is well-known to act as a potent stabilizer of the metal center and has allowed the isolation of species which, formula-wise, have the appearance of carrying the metal in low or exotic oxidation states.[6,11−13] However, the low *formal* oxidation state of some of these complexes may be deceiving since the ligand can accommodate up to three electrons in the delocalized *p*-system.[8] Therefore, an internal charge-transfer process may occur which results in a higher *actual* metal oxidation state.[6] Remarkably however, the reactivity of these "low-valent" metal centers is not quenched, given that dinitrogen complexes of this particular ligand system have been isolated for both vanadium[12] and iron.[13] This is an indication that intermediate reduced species can be stabilized while preserving their high reactivity. In the case of the bis-iminopyridine Fe catalyst, the oxidation state of the metal in the catalytically active species has not been conclusively determined. Based on Mossbauer and EPR studies of the pre-catalyst, it was argued that the active species may involve the trivalent oxidation state of Fe.[14] This conclusion was debated by Talsi et al., who suggested, on the basis of ^{1}H NMR, ^{2}H NMR, and EPR studies, the formation of a paramagnetic Fe(II) alkyl bridging the Al cocatalyst.[15] In addition to oxidation state, the spin multiplicity, in relation to the coordination number, also seems to play an important role in determining high activity. Calculations on the catalytically active species in the Fe catalyst, assumed to be either a cationic $[LFeR]^+$ complex[16] or a neutral LFeMe-(μMe)$_2$AlMe$_2$ species,[17] have led to a debate concerning the spin state of the metal center. Recent observations by Chirik on the catalytic activity of (diimine)FeR$_2$ complexes[18] lead to the tentative conclusion that the combination of high-spin state and tetracoordination may cause divalent Fe alkyls to be poorly active catalyst precursors due to the absence of empty orbitals available for olefin binding. Conversely, the recent isolation of cationic and divalent organoiron species has established the competency of cationic Fe(II) alkyls as polymerization catalysts.[18c]

The last point is the stability of the M−C bond. This issue, which is obviously central to catalyst behavior and activity, is particularly relevant in the case of the Fe catalyst. Organo-iron compounds are reasonably well established, including complexes of diamines and diimines, the latter being closely related to this work.[18] These species, however, display either poor stability toward reduction to the mono-[18] or zerovalent state or substantially diminished catalytic activity.[19] Yet, organo-iron complexes produce polymers when activated by MAO and Lewis acids. Although the stability of the Fe−C bond may be greatly increased by using ancillary ligands such as phosphines[19m−o] or cyclopentadienyl and CO,[19a] this practice usually quenches the reactivity of the metal center. It is therefore conceivable that, given the outstanding activity of the bis-iminopyridine Fe catalyst, the ligand provides the M−C bond with the appropriate stability to disfavor termination pathways while maintaining the high reactivity necessary for catalytic efficiency.

The aim of this study was to understand the chemistry of the Fe−C functionality in the bis-iminopyridine Fe catalyst {2,6-[2,6-(*i*-Pr)$_2$PhN═C(CH$_3$)]$_2$(C$_5$H$_3$N)}FeCl$_2$. Given the complexity of the behavior of this noninnocent ligand and its frequent involvement in the reactivity of the metal carbon bond, it is nearly impossible at this stage to reasonably argue about the true nature of the catalytically active species. Contrary to the other metal complexes mentioned above, in which alkylation processes have allowed the isolation of species that provide important mechanistic hints and partially unveil the complexity of this chemistry,[2−4,9,10,20] a crystallographically characterized organo-iron active intermediate has been isolated in only one case.[18c]

Herein, we describe the results of the alkylation of the bis-iminopyridine-FeCl$_2$ catalyst with R−Li [R = CH$_2$Si(CH$_3$)$_3$]. The choice of this particular alkylating agent was advised by the well-known stability of its organometallic derivatives.

Experimental Section

All operations were performed either under a nitrogen atmosphere using standard Schlenk techniques or in a purified nitrogen-filled drybox. The THF complex of FeCl$_2$ was prepared according to the standard procedure. The ligand 2,6-[2,6-(*i*-Pr)$_2$PhN═C(CH$_3$)]$_2$(C$_5$ H$_3$N),[1] the mono-[7] and di-deprotonated[6,9] derivatives, and LiCH$_2$Si(CH$_3$)$_3$[21] were prepared following published procedures. Infrared spectra were recorded on a Mattson 9000 and Nicolet 750-Magna FT-IR instrument from Nujol mulls prepared in a drybox. Samples for magnetic susceptibility measurements were weighed inside a drybox equipped with an analytical balance and sealed into calibrated tubes, and the measurements were carried out at room temperature with a Gouy balance (Johnson Matthey). Magnetic moments were calculated following standard methods, and corrections for underlying diamagnetism were applied to the data. Elemental analyses were performed on a Perkin-Elmer 2400 CHN analyzer. Data for X-ray crystal structure determinations were obtained with a Bruker diffractometer equipped with a Smart CCD area detector.

(11) de Bruin, B.; Bill, E.; Bothe, E.; Weyhermueller, T.; Wieghardt, K. *Inorg. Chem.* **2000**, *39*, 2936.
(12) Vidyaratne, I.; Gambarotta, S.; Korobkov, I.; Budzelaar, P. H. M. *Inorg. Chem.* **2005**, *44*, 1187.
(13) Bart, S. C.; Lobkovsky, E.; Chirik, P. J. *J. Am. Chem. Soc.* **2004**, *126*, 13794.
(14) Britovsek, G. J. P.; Clentsmith, G. K. B.; Gibson, V. C.; Goodgame, D. M. L.; McTavish, S. J.; Pankhurst, Q. A. *Catal. Commun.* **2002**, *3*, 207.
(15) (a) Bryliakov, K. P.; Semikolenova, N. V.; Zudin, V. N.; Zakharov, V. A.; Talsi, E. P. *Catal. Commun.* **2004**, *5*, 45. (b) Bryliakov, K. P.; Semikolenova, N. V.; Zakharov, V. A.; Talsi, E. P. *Organometallics* **2004**, *23*, 5375.
(16) (a) Deng, L.; Margl, P.; Ziegler, T. *J. Am. Chem. Soc.* **1999**, *121*, 6479. (b) Griffiths, E. A. H.; Britovsek, G. J. P.; Gibson, V. C.; Gould, I. R. *Chem. Commun.* **1999**, 1333. (c) Khoroshun, D. V.; Musaev, D. G.; Vreven, T.; Morokuma, K. *Organometallics* **2001**, *20*, 2007.
(17) Zakharov, I. I.; Zakharov, V. A. *Macromol. Theory Simul.* **2004**, *13*, 583.
(18) (a) Bart, S. C.; Hawrelak, E. J.; Schmisseur, A. K.; Lobkovsky, E.; Chirik, P. J. *Organometallics* **2004**, *23*, 237. (b) Bouwkamp, M. W.; Bart, S. C.; Hawrelak, E. J.; Trovitch, R. J.; Lobkovsky, E.; Chirik, P. J. *Chem. Commun*. **2005**, 3406. (c) Bowkamp, M. W.; Lobkovsky, E.; Chirik, P. J. *J. Am. Chem. Soc*. **2005**, *127*, 9660.
(19) (a) Kerber, R. C. *Comprehensive Organometallic Chemistry II*; Abel, E. W., Stone, F. G. A., Wilkinson, G., Eds.; Pergamon, New York, 1995. (b) Machelett, B. *Z. Chem.* **1976**, *16*, 116. (c) Mueller, H.; Seidel, W.; Goerls, H. *J. Organomet. Chem.* **1993**, *445*, 133. (d) Klose, A.; Solari, E.; Floriani, C.; Chiesi-Villa, A.; Rizzoli, C.; Re, N. *J. Am. Chem. Soc.* **1994**, *116*, 9123. (e) Seidel, W.; Mueller, H.; Goerls, H. *Angew. Chem., Int. Ed.* **1995**, *34*, 325. (f) Wehmschulte, R. J.; Power, P. P. *Organometallics* **1995**, *14*, 3264. (g) Viefhaus, T.; Schwarz, W.; Hubler, K.; Locke, K.; Weidlein, J. *Z. Anorg. Allg. Chem*. **2001**, *627*, 715. (h) Holland, P. L.; Cundari, T. R.; Perez, L. L.; Eckert, N. A.; Lachicotte, R. J. *J. Am. Chem. Soc.* **2002**, *124*, 14416. (i) Smith, J. M.; Lachicotte, R. J.; Holland, P. L. *Organometallics* **2002**, *21*, 4808. (j) Sciarone, T. J. J.; Meetsma, A.; Hessen, B.; Teuben, J. H. *Chem. Commun.* **2002**, 1580. (k) Kisko, J. L.; Hascall, T.; Parkin, G. *J. Am. Chem. Soc.* **1998**, *120*, 10561. (l) Fryzuk, M. D.; Leznoff, D. B.; Ma, E. S. F.; Rettig, R. J.; Young, V. G. *Organometallics* **1998**, *17*, 2313. (m) Hermes, A. R.; Girolami, G. S. *Organometallics*, **1987**, *6*, 763. (n) Chatt, J.; Shaw, B. L. *J. Chem. Soc.* **1961**, 285. (o) Seidel, V. W.; Lattermann, K.-J. *Z. Anorg. Allg. Chem.* **1982**, *488*, 69. (p) Spencer, L. P.; Altwer, R.; Wei, P.; Gelmini, L.; Gauld, J.; Stephan, D. W. *Organometallics* **2003**, *22*, 3841. (q) Mueller, H.; Seidel, W.; Goerls, H. *Z. Anorg. Allg. Chem.* **1996**, *622*, 756. (r) Hill, D. H.; Sen, A. *J. Am. Chem. Soc.* **1988**, *110*, 1651.
(20) (a) Kooistra, T. M.; Knijnenburg, Q.; Smits, J. M. M.; Horton, A. D.; Budzelaar, P. H. M.; Gal, A. W. *Angew. Chem., Int. Ed.* **2001**, *40*, 4719. (b) Gibson, V. C.; Humphries, M. J.; Tellmann, K. P.; Wass, D. F.; White, A. J. P.; Williams, D. J. *Chem. Commun.* **2001**, 2252. (c) Humphries, M. J.; Tellmann, K. P.; Gibson, V. C.; White, A. J. P.; Williams, D. J. *Organometallics* **2005**, *24*, 2039.
(21) Tessier-Youngs, C.; Beachley, O. T., Jr. *Inorg. Synth*. **1986**, *24*, 95.

Preparation of {2,6-[2,6-(*i*-Pr)$_2$PhN═C(CH$_3$)]$_2$(C$_5$H$_3$N)}FeCl$_2$. A suspension of 2,6-[2,6-(*i*-Pr)$_2$PhN═C(CH$_3$)]$_2$(C$_5$H$_3$N) (2.05 g, 4.26 mmol) in THF was added to a suspension of FeCl$_2$(THF)$_{1.5}$ (1.00 g, 4.26 mmol) in THF, and the resulting dark blue mixture was stirred overnight. After evaporating the THF, the residue was dissolved in an appropriate amount of CH_2Cl_2, concentrated, and layered with hexane. Dark blue crystals of the Fe-bis-iminopyridine-dichloride starting complex were grown while sitting at room temperature for 2 days. Although this procedure is very similar to published procedures,[1] this synthesis strictly avoids the use of water or alcohols and, as such, ensures a "dry" starting complex for further reactions.

Preparation of {2,6-[2,6-(*i*-Pr)$_2$PhN═C(CH$_3$)]$_2$-(2-CH$_2$SiMe$_3$)}-(C$_5$H$_3$N)Fe(CH$_2$SiMe$_3$) (1). A suspension of FeCl$_2$(THF)$_{1.5}$ (0.200 g, 0.85 mmol) and 2,6-[2,6-(*i*-Pr)$_2$PhN═C(CH$_3$)]$_2$(C$_5$H$_3$N) (0.410 g, 0.85 mmol) in approximately 10 mL of THF was stirred for 4 h affording the usual dark-blue color. The suspension was cooled to −35 °C and mixed with a cooled solution of LiCH$_2$SiMe$_3$ (0.168 g, 1.78 mmol) in THF. The color of the solution instantly changed from royal blue to dark reddish-orange upon mixing. The solution was stirred for approximately 1 min to ensure complete mixing and evaporated to dryness, maintaining a cold temperature throughout the procedure. Cold hexane was added to the dark brown residue, and a dark reddish-orange suspension was centrifuged to remove a substantial amount of insoluble material. The resulting solution was allowed to stand at −35 °C for 1 day, upon which time the mother liquor was removed from small dark crystals (recognized later as a small amount of **2**), concentrated, and put back in the freezer for 2 days, resulting in the crystallization of **1** as dark red crystals (0.212 g, 0.30 mmol, 35% yield). Anal. Calcd (found) for C$_{41}$H$_{65}$FeN$_3$Si$_2$: C, 69.16 (69.05); H, 9.20 (9.18); N, 5.90 (5.87). IR (Nujol mull, cm^{-1}): ν 3066 (w), 2929 (s), 1614 (m), 1568 (s), 1498 (s), 1363 (m), 1352 (m), 1321 (s), 1288 (m), 1242 (m), 1195 (m), 1143 (m), 1099 (w), 1056 (w), 1043 (w), 970 (w), 946 (w), 937 (w), 881 (s), 850 (s,b), 813 (m,b), 773 (m), 721 (m,b), 700 (m) [μ_{eff} = 5.6 μ_B].

Preparation of {2,6-[2,6-(*i*-Pr)$_2$PhN═C(CH$_3$)]$_2$}(C$_5$H$_3$N)Fe(CH$_2$-SiMe$_3$)$_2$ (2). *Method A.* The preparation was carried out as above except that the remaining hexane-insoluble solids were dissolved in ether. The color became dark purple, and the mixture was centrifuged to separate a dark purple solution from a small amount of colorless solids. The ether solution was concentrated and kept at −35 °C for 2 days, upon which crystals of **2** suitable for X-ray analysis were isolated (0.180 g, 0.25 mmol, 30% yield). Anal. Calcd (found) for C$_{41}$H$_{65}$FeN$_3$Si$_2$: C, 69.16(69.13); H, 9.20(9.15); N, 5.90(5.83). IR (Nujol mull, cm^{-1}): ν 2931 (s), 2865 (s), 1645 (w), 1585 (w), 1548 (w), 1282 (s), 1259 (m), 1263 (s), 1193 (w), 1155 (m), 1135 (m), 1110 (w), 1097 (w), 973 (s), 916 (w), 894 (w), 850 (s,b), 823 (s), 775 (m), 727 (m,b) [μ_{eff} = 5.6 μ_B].

Method B. A solution of LiCH$_2$SiMe$_3$ (0.168 g, 1.78 mmol) in ether (5 mL) was added to a suspension of FeCl$_2$(THF)$_{1.5}$ (0.200 g, 0.85 mmol) in ether (5 mL) at −35 °C. The mixture began to turn yellow with swirling. The mixture was kept at −35 °C with periodic swirling for approximately 2 min. The resulting brownish-yellow suspension was added to a cooled suspension of 2,6-[2,6-(*i*-Pr)$_2$PhN═C(CH$_3$)]$_2$-(C$_5$H$_3$N) (0.410 g, 0.85 mmol) in ether (10 mL). The color instantly became dark purple, and the mixture was stirred for 2 min to ensure complete mixing. The reaction was then centrifuged to remove a dark purple solution from white precipitates. Upon concentrating and freezing at −35 °C, dark purple block crystals of **2** were obtained (0.357 g, 0.50 mmol, 59% yield).

Method C. A solution of LiCH$_2$SiMe$_3$ (0.170 g, 1.80 mmol) in THF (5 mL) was added to a suspension of {2,6-[2,6-(*i*-Pr)$_2$PhN═C(CH$_3$)]$_2$-(C$_5$H$_3$N)}FeCl$_2$ (0.500 g, 0.82 mmol) in 10 mL of THF at −35 °C. The color slowly changed from dark blue to dark brownish-red, and the solids slowly went into solution upon stirring. After stirring for approximately 30 min, the solvent was evaporated and cold hexane was added to the brown residue. The resulting suspension was centrifuged, and a dark olive-green solution (from which **4** crystallized) was separated from the dark precipitates. Diethyl ether was added to the precipitates, and the solution was centrifuged to separate a dark purple solution from white precipitates. Concentration of the solution and standing in the freezer for 2 days afforded crystals of **2** (0.304 g, 0.427 mmol, 52% yield).

Preparation of {2-[2,6-(*i*-Pr)$_2$PhN═C(CH$_3$)]-6-[2,6-(*i*-Pr)$_2$PhNC-(CH$_3$)(CH$_2$SiMe$_3$)](C$_5$H$_3$N)}Fe(CH$_2$SiMe$_3$) (3). A procedure identical to that described for complex **1** was followed. Crystals of **3** grew out of the same hexane solution as **1** but could be physically separated with the help of a stereomicroscope due to their very distinct rectangular shape (0.055 g, 0.08 mmol, 10% yield). Anal. Calcd (found) for C$_{41}$H$_{65}$-FeN$_3$Si$_2$: C, 69.16 (69.10); H, 9.20 (9.18); N, 5.90 (5.87).

Transformation of 3 to 2. Addition of diethyl ether to crystals of **3** (0.055 g, 0.08 mmol) afforded a dark purple solution from which dark purple crystals of **2** were isolated after freezing at −35 °C for 2 days (0.035 g, 0.05 mmol, 62% yield).

Preparation of {2,6-[2,6-(*i*-Pr)$_2$PhN−C═(CH$_2$)]$_2$(C$_5$H$_3$N)}Fe(μ-Cl)Li(THF)$_3$ (4). *Mehod A.* To a suspension of {2,6-[2,6-(*i*-Pr)$_2$PhN═C(CH$_3$)]$_2$(C$_5$H$_3$N)}FeCl$_2$ (0.500 g, 0.82 mmol) in THF (10 mL) a solution of LiCH$_2$SiMe$_3$ (0.170 g, 1.80 mmol) also in THF (5 mL) was added at −35 °C. The color slowly changed from dark blue to dark brownish-red, and the solids slowly went into solution with stirring. After stirring for approximately 30 min, the solvent was evaporated and cold hexane was added to the brown residue. The resulting suspension was centrifuged, and a dark olive-green solution was separated from dark precipitates (identified as **2** upon recrystallization in ether 65% yield). The solution was placed in the freezer overnight, and then the mother liquor was removed from a small amount of crystallized **2** and placed back in the freezer. Dark orange crystals of **4** were grown from the hexane solution after standing at −35 °C for 2 days (0.098 g, 0.12 mmol, 15% yield). Anal. Calcd (found) for C$_{45}$H$_{66}$-ClFeLiN$_3$O$_3$: C, 67.96 (67.93); H, 8.37 (8.31); N, 5.28 (5.24). IR (Nujol mull, cm^{-1}): ν 2918 (s), 2854 (s), 1644 (m), 1572 (s), 1322 (m), 1279 (s), 1249 (m), 1236 (s), 1210 (w), 1193 (w), 1154 (m), 1134 (m), 1107 (m,b), 1047 (s), 1005 (m), 972 (s), 890 (m), 848 (s,b), 822 (s), 773 (s), 727 (s) [μ_{eff} = 5.8 μ_B].

Method B. {[2,6-{[2,6-(*i*-Pr)$_2$C$_6$H$_3$]N−C═(CH$_2$)}$_2$(C$_5$H$_3$N)]Li(THF)}-{Li(THF)$_4$} (0.727 g, 0.85 mmol) was added to a suspension of FeCl$_2$-(THF)$_{1.5}$ (0.200 g, 0.85 mmol) in THF (35 mL) at −35 °C. The color of the suspension turned instantly dark orange-brown. After stirring for approximately 30 min, the solvent was evaporated to dryness and the resulting mass was washed with ether to remove a dark green solution. The residual solid wase dissolved in toluene, centrifuged to a dark greenish-brown solution, concentrated, and placed in the freezer. Dark orange crystals of **4** were obtained upon standing at −35 °C for 2 days (0.379 g, 0.48 mmol, 56% yield).

Preparation of [{2,6-[2,6-(*i*-Pr)$_2$PhN−C═(CH$_2$)]$_2$(C$_5$H$_3$N)}FeCH$_2$Si-(CH$_3$)$_3$][Li(THF)$_4$] (6). A solution of LiCH$_2$SiMe$_3$ (0.168 g, 1.78 mmol) in ether was added to a suspension of FeCl$_2$(THF)$_{1.5}$ (0.200 g, 0.85 mmol) in ether at −35 °C. The mixture was stirred for approximately 2 min, upon which time the color gradually became darker yellow-brown. At this time, a solution of {2-[2,6-(*i*-Pr)$_2$PhN−C═(CH$_2$)]-6-[2,6-(*i*-Pr)$_2$PhN−CCH$_3$](C$_5$H$_3$N)}Li(THF) (0.476 g, 0.85 mmol) in ether, also kept at −35 °C, was added. The color of the mixture became dark royal blue, and stirring was continued for 1 h. The solvent was removed in vacuo, and the residual mass was dissolved in THF. The solution was centrifuged and separated from a small amount of dark precipitate. Concentration and layering with hexane afforded, after standing for 2 days, reddish-brown crystals of **6** (0.430 g, 0.47 mmol, 55% yield). Anal. Calcd (found) for C$_{53}$H$_{86}$SiN$_3$FeLiO$_4$: C, 69.18 (68.77); H, 9.42 (9.68); N, 4.57 (5.01). IR (Nujol mull, cm^{-1}): ν 2952 (s), 2855 (s), 1561 (s), 1523 (w), 1468 (s), 1434 (m), 1377 (m), 1367 (m), 1356 (m), 1320 (m), 1309 (w), 1283 (w), 1252 (m), 1228 (w), 1209 (w), 1176 (w), 1125 (w), 1101 (w), 1083 (w), 1040 (s), 1003

Table 1. Crystal Data

	1	3	4	6
formula	$C_{41}H_{65}FeN_3Si_2$	$C_{41}H_{65}FeN_3Si_2$	$C_{45}H_{66}ClFeLiN_3O_3$	$C_{53}H_{86}N_3FeLiO_4Si$
M_w	711.99	711.99	795.25	920.13
crystal system	monoclinic	triclinic	monoclinic	monoclinic
space group	$P2(1)/n$	$P\bar{1}$	$P2(1)/n$	$P2(1)/c$
a (Å)	9.8426(12)	9.610(3)	11.574(3)	15.998(19)
b (Å)	18.821(2)	10.865(3)	18.331(5)	27.61(3)
c (Å)	22.748(3)	22.115(7)	21.787(5)	24.90(3)
α (deg)	90	89.135(5)	90	90
β (deg)	91.684(2)	85.805(6)	96.094(5)	97.75(2)
γ (deg)	90	66.610(5)	90	90
V (Å^3)	4212.1(9)	2113.5(12)	4596.3(19)	10 902(22)
Z	4	2	4	4
radiation (Kα, Å)	0.710 73	0.710 73	0.710 73	0.710 73
T (K)	206(2)	208(2)	208(2)	213
D_{calcd} (g cm^{-3})	1.124	1.119	1.149	1.121
μ_{calcd} (mm^{-1})	0.445	0.443	0.425	0.342
F_{000}	1548	772	1708	4000
R, R_w[2]	0.0623, 0.1399	0.0721, 0.1272	0.0783, 0.1540	0.0688, 0.1518
GOF	1.036	1.011	1.065	1.008

Table 2. Selected Bond Distances and Angles

1	3	4	5	6
Fe−N(1) = 2.224(3)	Fe−N(1) = 2.433(3)	Fe−N(1) = 2.013(6)	Fe−C(34) = 2.05	Fe−N(1) = 2.094(4)
Fe−N(2) = 2.015(2)	Fe−N(2) = 2.130(3)	Fe−N(2) = 2.095(6)	N(1)−C(2) = 1.31	Fe−N(2) = 2.138(4)
Fe−N(3) = 2.160(3)	Fe−N(3) = 1.960(3)	Fe−N(3) = 2.022(6)	C(1)−C(2) = 1.50	Fe−N(3) = 2.078(4)
Fe−C(41) = 2.036(3)	Fe−C(38) = 2.045(4)	Fe−Cl = 2.318(2)	N(3)−C(8) = 1.31	Fe−C(34) = 2.068(5)
C(1)−C(2) = 1.499(5)	C(1)−C(2) = 1.499(6)	N(1)−C(2) = 1.380(9)	C(8)−C(9) = 1.49	N(1)−C(2) = 1.360(6)
N(2)−C(3) = 1.473(4)	N(3)−C(8) = 1.477(5)	C(1)−C(2) = 1.362(10)		N(3)−C(8) = 1.354(6)
C(3)−C(4) = 1.516(4)	C(8)−C(9) = 1.533(5)	N(3)−C(8) = 1.375(9)		C(1)−C(2) = 1.337(7)
C(4)−C(5) = 1.338(5)	N(1)−Fe−N(2) = 69.27(12)	C(8)−C(9) = 1.344(10)		C(8)−C(9) = 1.356(7)
C(5)−C(6) = 1.429(5)	N(1)−Fe−N(3) = 145.82(13)	Cl−Li = 2.362(13)		N(1)−Fe−N(3) = 145.67(15)
C(6)−C(7) = 1.371(4)	N(1)−Fe−C(38) = 99.55(15)	N(1)−Fe−N(2) = 75.7(3)		N(2)−Fe(1)−C(34) = 155.4(2)
C(7)−N(2) = 1.366(4)	N(2)−Fe−N(3) = 78.49(13)	N(1)−Fe−N(3) = 151.3(3)		N(1)−Fe−C(34) = 107.1(2)
C(8)−C(9) = 1.489(5)	N(2)−Fe−C(38) = 156.75(16)	N(1)−Fe−Cl = 104.25(19)		N(2)−Fe−N(3) = 74.08(16)
N(1)−Fe−N(2) = 75.94(10)	N(3)−Fe−C(38) = 114.62(16)	N(2)−Fe−N(3) = 75.7(3)		N(1)−C(2)−C(1) = 127.6(5)
N(1)−Fe−N(3) = 121.88(10)		N(2)−Fe−Cl = 177.48(18)		Fe−C(34)−Si(1) = 128.6(3)
N(1)−Fe−C(41) = 115.74(13)		N(3)−Fe−Cl = 104.44(19)		
N(2)−Fe−N(3) = 78.37(11)		Fe−Cl−Li = 171.0(4)		
N(2)−Fe−C(41) = 140.44(13)				
N(3)−Fe−C(41) = 117.27(13)				

(m), 968 (w), 935 (w), 916 (w), 887 (s), 868 (s), 812 (m), 771 (m), 760 (m), 746 (m), 722 (m) [μ_{eff} = 5.6 μ_B].

X-ray Crystallography. All of the compounds **1** to **6** consistently yielded crystals that diffracted weakly, and the results presented are the best of several trials. The crystals were mounted on thin glass fibers using paraffin oil and cooled to the data collection temperature. Data were collected on a Bruker AXS SMART 1k CCD diffractometer. Data for the compounds **1** and **6** were collected with a sequence of 0.3° ω scans at 0°, 120°, and 240° in φ. To obtain acceptable redundancy data for compound **3**, the sequence of 0.3° ω scans at 0°, 90°, 180°, and 270° in φ was used. Initial unit cell parameters were determined from 50 data frames collected at the different sections of the Ewald sphere. Semiempirical absorption corrections based on equivalent reflections were applied.[22] Systematic absences in the diffraction dataset and unit-cell parameters were consistent with monoclinic $P2_1/n$ for **1**, orthorhombic, triclinic $P\bar{1}$ for **3**, monoclinic $P2_1/n$ for **4**, and monoclinic $P2_1/c$ for **6**. Solutions in centrosymmetric space groups for all of the compounds yielded chemically reasonable and computationally stable results of refinement. The structures were solved by direct methods, completed with difference Fourier synthesis, and refined with full-matrix least-squares procedures based on F^2. The compound molecules were located in common positions in the structures of all the complexes. All non-hydrogen atoms were refined with anisotropic displacement coefficients. All hydrogen atoms were treated as idealized contributions. All scattering factors are contained in several versions of the SHELXTL program library, with the latest version used being v.6.12.[23] Crystallographic data and relevant bond distances and angles are reported in Tables 1 and 2.

Calculations. Density functional calculations on model complexes (see below) were performed with the TURBOMOLE program[24] in combination with the OPTIMIZE routine of Baker and co-workers.[25] All relevant structures were fully optimized as minima or transition states at the restricted or unrestricted b3-lyp[26] level, employing the standard SV(P) basis sets.[27] All stationary points were characterized by vibrational analyses using analytic or numerical second derivatives, and thermal corrections (ZPE, enthalpy, entropy; 273K, 1 bar) were calculated from these using standard formulas of statistical thermodynamics. Improved electronic energies were calculated at the SV(P)

(22) Blessing, R. *Acta Crystallogr.* **1995**, *A51*, 33.

(23) Sheldrick, G. M. Bruker AXS: Madison, WI, 2001.

(24) (a) Ahlrichs, R.; Baer, M.; Haeser, M.; Horn, H.; Koelmel, C. *Chem. Phys. Lett.* **1989**, *162*, 165. (b) Treutler, O.; Ahlrichs, R. *J. Chem. Phys.* **1995**, *102*, 346. (c) Ahlrichs, R.; et al. *Turbomole*; version 5, January 2002. Theoretical Chemistry Group, University of Karlsruhe.

(25) Baker, J. *J. Comput. Chem.* **1986**, *7*, 385; *PQS*, version 2.4; Parallel Quantum Solutions, Fayetteville, Arkansas, USA, 2001; the Baker optimizer is available separately from PQS upon request.

(26) (a) Lee, C.; Yang, W.; Parr, R. G. *Phys. Rev. B* **1988**, *37*, 785. (b) Becke, A. D. *J. Chem. Phys.* **1993**, *98*, 1372. (c) Becke, A. D. *J. Chem. Phys.* **1993**, *98*, 5648. Note that the Turbomole functional "b3-lyp" is not identical to the Gaussian "B3LYP" functional.

(27) Schaefer, A.; Horn, H.; Ahlrichs, R. *J. Chem. Phys.* **1992**, *97*, 2571.

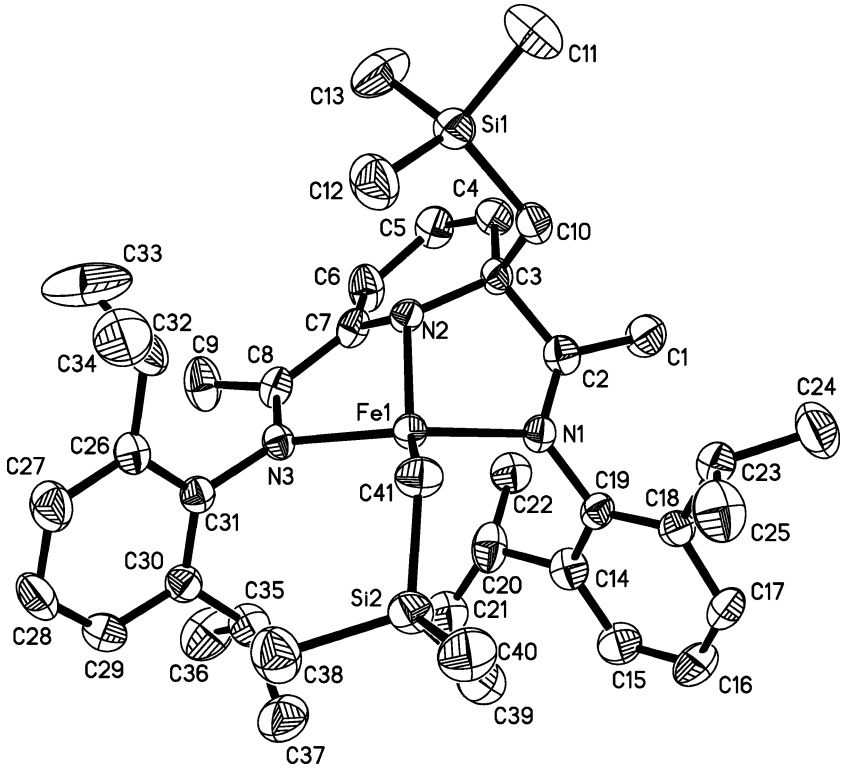

Figure 1. Thermal ellipsoid plot for **1** with the ellipsoids drawn at the 30% probability level

Scheme 1

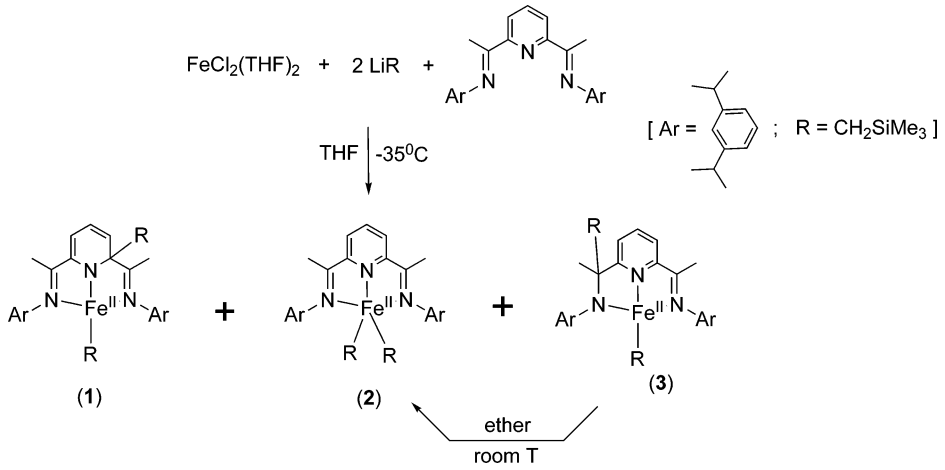

optimized geometries using the TZVPP basis set on all atoms;[28] these improved energies were combined with the (u)b3-lyp/sv(p) thermal corrections to arrive at the final free energies.

Extensive calculations were carried out on model complex L′$FeMe_2$ (**2a**) and its alkyl-shifted isomers [L′-2-Me]FeMe (**1a**) and [L′-*i*-Me]-FeMe (**3a**), where L′ is a model ligand bearing only Me groups at the imine nitrogens. In addition, an isomer [L′−N−Me]FeMe (the product of alkyl migration to the pyridine nitrogen) was included because this might be an intermediate in alkyl transfers between metal and ligand. Finally, the Fe^{I} complex L′FeMe (**5a**) was included as a model for half of complex **5**. Geometries for spin states from $S = 0$ to 3 (for Fe^{II}) or $^1/_2$ to $^5/_2$ (for Fe^{I}) were fully optimized for each of the above-mentioned species. For the triplet and quintet states only, the geometries of the full complexes **1**, **2**, **3**, and [L−N−R]FeR (L−N−R = pyridine ring N-alkylated; R = CH_2SiMe_3) were also fully optimized; larger basis sets and thermal corrections were not feasible here.

(28) Schaefer, A.; Huber, C.; Ahlrichs, R. *J. Chem. Phys.* **1994**, *100*, 5829.

Results and Discussion

The reaction of $LiCH_2SiMe_3$ with the dark-blue 2,6-[2,6-(*i*-$Pr)_2PhN{=}C(CH_3)]_2(C_5H_3N)FeCl_2$, prepared in situ by reacting the neutral 2,6-[2,6-(*i*-$Pr)_2PhN{=}C(CH_3)]_2(C_5H_3N)$ ligand with $FeCl_2(THF)_{1.5}$, was carried out in THF at −35 °C (Scheme 1). Dark-burgundy crystals of the divalent {2,6-[2,6-(*i*-$Pr)_2PhN{=}C(CH_3)]_2$-2-CH_2SiMe_3}$(C_5H_3N)Fe(CH_2SiMe_3)$ (**1**) were isolated after separation from the insoluble materials and fractional crystallization in pure hexane. In turn, the hexane-insoluble fraction was recrystallized from cold ether affording large, dark-purple crystals of {2,6-[2,6-(*i*-$Pr)_2PhN{=}C(CH_3)]_2$}$(C_5H_3N)Fe(CH_2SiMe_3)_2$ (**2**) (Scheme 1). The formation of the two complexes is a perfectly reproducible phenomenon under the reaction conditions described in the Experimental Section. The formulas and connectivity of both complexes have been elucidated by X-ray crystal structures (Figures 1 and 2).

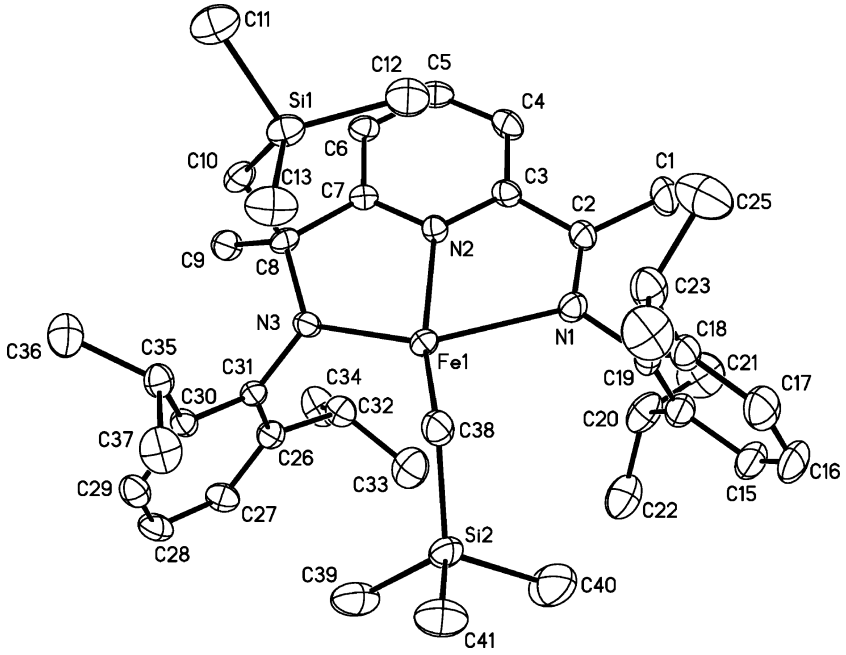

Figure 2. Thermal ellipsoid plot for **3** with the ellipsoids drawn at the 30% probability level.

Complex **1** consists of an Fe atom coordinated to the three nitrogen atoms of the ligand system [Fe−N(1) = 2.224(3) Å, Fe−N(2) = 2.015(2) Å, Fe−N(3) = 2.160(3) Å] which has been alkylated at one of the two pyridine ring *ortho*-positions (Figure 1). One silylated-alkyl group is also attached to Fe [Fe−C(41) = 2.036(3) Å], providing the metal center with a severely distorted tetrahedral coordination geometry [N(1)−Fe−N(2) = 75.94(10)°, N(1)−Fe−N(3) = 121.88(10)°, N(1)−Fe−C(41) = 115.74(13)°, N(2)−Fe−N(3) = 78.37(11)°, N(2)−Fe−C(41) = 140.44(13)°, N(3)−Fe−C(41) = 117.27(13)°]. The consequence of the pyridine ring alkylation and resulting loss of aromaticity can be noticed in the ring deviation from planarity and the expected variation in bond lengths [N(2)−C(3) = 1.473(4) Å, C(3)−C(4) = 1.516(4) Å, C(4)−C(5) = 1.338(5) Å, C(5)−C(6) = 1.429(5) Å, C(6)−C(7) = 1.371(4) Å, C(7)−N(2) = 1.366(4) Å]. The other geometrical parameters of the ligand do not show significant features and are comparable to those of the vanadium catalyst that underwent a similar fate upon alkylation with MAO.[2]

Single crystals of **2** displayed identical cell parameters and structure to those recently reported by Chirik while this work was in progress.[18b] The formation of **1** is the result of two distinct processes. The first is the alkylation of the pyridine ring *ortho* position. The *ortho* alkylation has a major impact on the molecular structure since the consequent anionization of the neutral ligand requires dissociation of one of the two chlorine atoms attached to the Fe atom with a decrease in the metal coordination number. The second process is a straightforward replacement of the remaining chlorine atom by the second alkylating agent. The connectivity, as summarized in Scheme 1, unambiguously assigns the divalent state to the Fe center. The magnetic moment of 5.6 μ_B measured at room temperature with the Gouy method is in the expected range[29] for the four-unpaired-electron configuration of high-spin d^6 Fe(II) and is in good agreement with the original observations by Brookhart and Gibson on the $FeCl_2$ adduct.[1c−d]

At first glance, the formation of complex **2** seems to be the result of a straightforward chlorine replacement of 2,6-[2,6-(*i*-Pr)$_2$PhN=C(CH$_3$)]$_2$(C$_5$H$_3$N)FeCl$_2$. However, the yield of **2** can be substantially improved (up to 30% increase), and the formation of **1** virtually was eliminated (it was no longer present among the products isolable from the reaction mixtures) when the reaction was carried out by inverting the order of addition of the reagents (beginning with a low-temperature reaction between $FeCl_2$ and RLi, followed by a low-temperature addition of the ligand). This suggests, as an alternative possibility, that the formation of **2** may also be the result of the direct reaction of RLi with free $FeCl_2$ *followed* by complexation of the diimine ligand. The presumed presence of free $FeCl_2$ in the reaction mixture leading to the mixture of **1** and **2** may be caused by a ligand dissociation equilibrium from 2,6-[2,6-(*i*-Pr)$_2$PhN=C(CH$_3$)]$_2$(C$_5$H$_3$N)FeCl$_2$, as observed for example in the chemistry of the lanthanides.[6,7c,9] This point is further substantiated by the observation that transmetalation reactions are readily obtainable with this ligand system. For example, simple mixing at room temperature of 2,6-[2,6-(*i*-Pr)$_2$PhN=C(CH$_3$)]$_2$(C$_5$H$_3$N)-$FeCl_2$ with $CoCl_2$ in THF affords the corresponding $CoCl_2$ adduct and $FeCl_2$ after 2 h of stirring at room temperature.[30] Another possibility is that the very poor solubility of both unreacted $FeCl_2$ and the complex could make the presence of $FeCl_2$ unavoidable during its in situ preparation. Even in this case, the room-temperature magnetic moment of **2** [μ_{eff} = 5.6 μ_B] compares well with that of both the starting 2,6-[2,6-(*i*-Pr)$_2$PhN=C(CH$_3$)]$_2$(C$_5$H$_3$N)FeCl$_2$[1c−d] and **1** thus confirming that the metal has remained in its divalent state. Finally, it should be observed that neither **1** nor **2** can be formed by reaction of RLi with the ligand *followed* by reaction with $FeCl_2$. The lithium alkyl Me_3SiCH_2Li instantly reacts at either room or low temperature to produce the dianionic form of the ligand

(29) Cotton, F. A.; Wilkinson, G. *Advanced Inorganic Chemistry*, 5th ed.; Wiley Interscience, New York, 1988.

(30) Scott, J. Gambarotta, S. Unpublished results.

Scheme 2

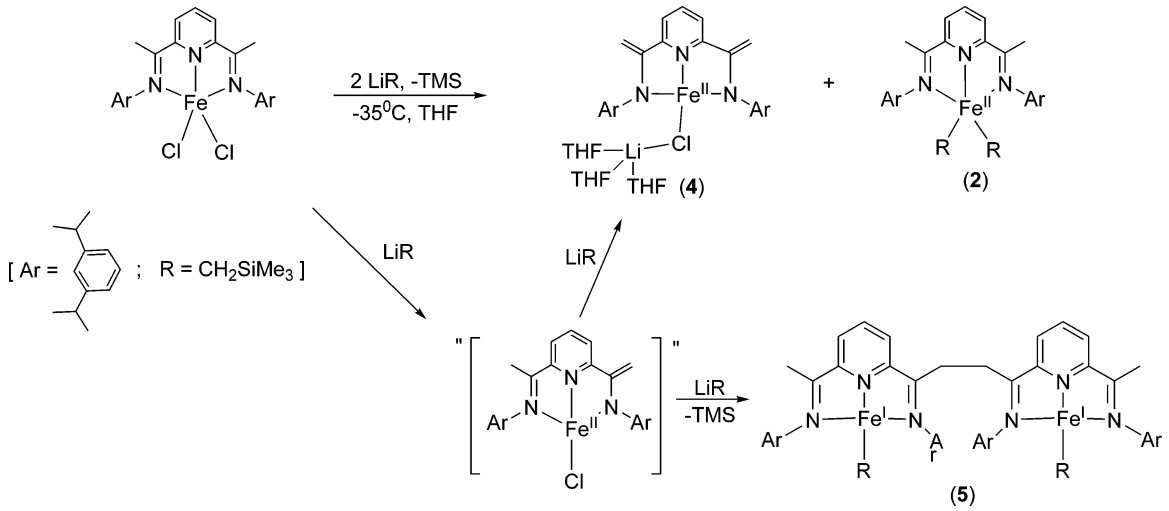

regardless of the stoichiometric ratio.[6,9] The resulting dianion forms a different product with $FeCl_2$ (see below).

We have observed that, during the formation of **1**, variable amounts of well-formed crystals of a similar color but different shape occasionally appeared, provided that the entire workup is carried out at a temperature kept below −20 °C. Manual separation of these crystals under microscope afforded the new complex {2-[2,6-(*i*-Pr)$_2$PhN═C(CH$_3$)]-6-[2,6-(*i*-Pr)$_2$PhNC(CH$_3$)-(CH$_2$SiMe$_3$)](C$_5$H$_3$N)}Fe(CH$_2$SiMe$_3$) (**3**) (Figure 2).

The structure of **3** consists of a tetracoordinate Fe atom surrounded by the ligand system which has undergone alkylation similar to the case of **1** (Figure 2). However, instead of being attached to the pyridine ring-*ortho* position, the alkyl is found connected to one of the two former imine C atoms. The coordination sphere of the metal center is defined by the three N atoms of the alkylated ligand system and the C atom of one alkyl group [Fe−N(1) = 2.433(3) Å, Fe−N(2) = 2.130(3) Å, Fe−N(3) = 1.960(3) Å, Fe−C(38) = 2.045(4) Å]. The coordination geometry of Fe is once again distorted tetrahedral [N(1)−Fe−N(2) = 69.27(12)°, N(1)−Fe−N(3) = 145.82(13)°, N(1)−Fe−C(38) = 99.55(15)°, N(2)−Fe−N(3) = 78.49(13)°, N(2)−Fe−C(38) = 156.75(16)°, N(3)−Fe−C(38) = 114.62-(16)°]. The alkylation of the ligand C_{imine} atom causes a substantial distortion and deviation from planarity in that region of the molecule. The quaternization of the former imine C atom reflects in bond distances and angles as expected for the disappearance of the conjugation [N(3)−C(8) = 1.477(5) Å, N(3)−C(8)−C(7) = 108.0(3)°]. The Fe−N distance is also shorter than the others as a result of the acquisition of anionic character of that particular N atom.

Similar to the case of **1** and **2**, the formation of this complex also requires the intervention of two alkyl groups. However, one has been attached to one of the two imine C atoms while the metal center bears the second. This implies that, similar to the case of **1**, the ligand is monoanionic and that the metal center is in the divalent state. During attempts to recrystallize **3** we have observed that the dark-burgundy color becomes purple when dissolved at room temperature in ether. Crystallization from ether afforded a good yield of **2**, thus indicating that simple dissolution of **3** in ether is sufficient for the conversion, which requires migration of the alkyl group from the imine carbon atom toward the metal center. In turn, this also indicates that, depending on the reaction conditions, **3** might be an intermediate in the formation of **2**, which apparently is thermodynamically more stable but kinetically less favored. No evidence could be found that **1** may be thermally transformed to **2** in either presence or absence of ethers.

The reaction of 2,6-[2,6-(*i*-Pr)$_2$PhN═C(CH$_3$)]$_2$(C$_5$H$_3$N)FeCl$_2$ with 2 equiv of LiCH$_2$SiMe$_3$ followed a surprisingly different course when it was carried out using the *analytically pure complex* resuspended in THF (Scheme 2), rather than the in-situ-generated species. In this case, we found no evidence for the formation of either **1** or **3**. The reaction, which is completely reproducible, afforded a substantial yield of **2** and a smaller amount of a new dark-orange byproduct {2,6-[2,6-(*i*-Pr)$_2$PhN−C═(CH$_2$)]$_2$(C$_5$H$_3$ N)}Fe(*μ*-Cl)Li(THF)$_3$ (**4**) which was isolated and purified by fractional crystallization.

Complex **4** can also be conveniently prepared (56% isolated crystalline material) via direct reaction of the dianionic form of the ligand (obtained either in situ or in crystalline form from the high yield reaction with 2 equiv of Me$_3$SiCH$_2$Li at either

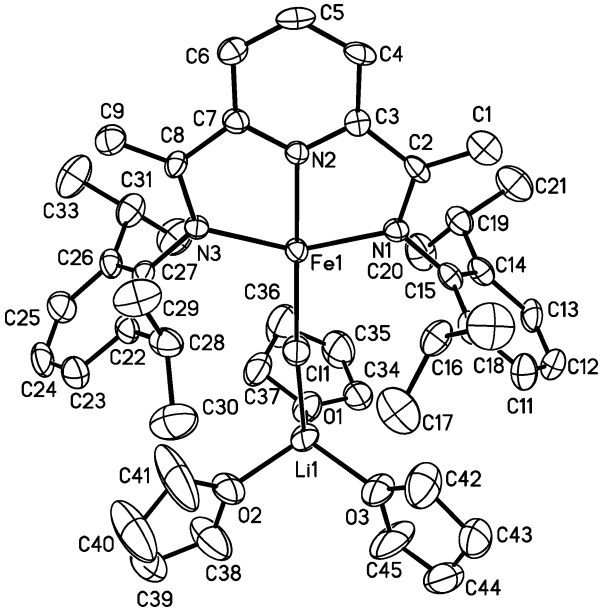

Figure 3. Thermal ellipsoid plot for **4** with the ellipsoids drawn at the 30% probability level

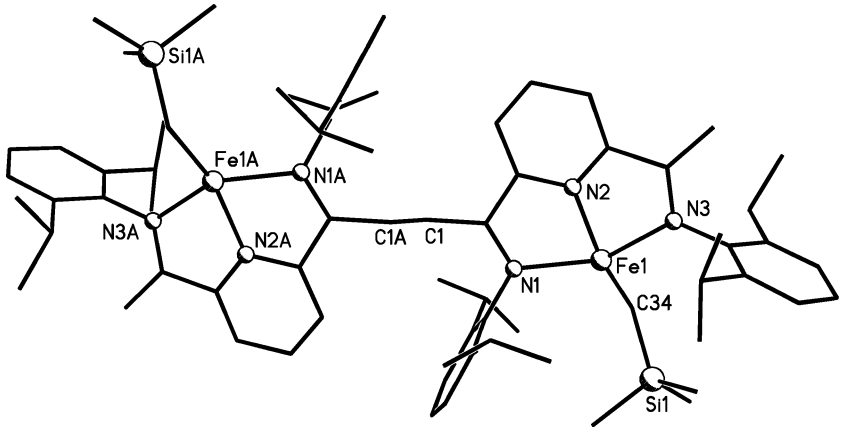

Figure 4. Ball and stick drawing of **5**.

low or room temperature) with $FeCl_2$. In all the reactions involving ligand deprotonation, it was always possible to detect formation of tetramethylsilane in the reaction mixtures by GC−MS experiments.

The molecule consists of a four-coordinate Fe atom (Figure 3) bonded to the three nitrogen atoms of the newly modified ligand [Fe−N(1) = 2.013(6) Å, Fe−N(2) = 2.095(6) Å, Fe−N(3) = 2.022(6) Å] and a chlorine atom [Fe−Cl = 2.318(2) Å]. The chlorine atom bridges one Li cation solvated by three molecules of THF [Cl−Li = 2.362(13) Å]. The Fe center is found in a slightly distorted square planar geometry [N(1)−Fe−N(2) = 75.7(3)°, N(2)−Fe−N(3) =75.7(3)°, N(3)−Fe−Cl = 104.44(19)°, Cl−Fe−N(1) = 104.25(19)°, N(1)−Fe−N(3) = 151.3(3)°, N(2)−Fe−Cl = 177.48(18)°]. The ligand system displays a very short distance between the C_{imine} and the C of the substituent [C(1)−C(2) = 1.362(10) Å, C(8)−C(9) = 1.344-(10) Å]. This typically indicates that the former Me group has been deprotonated with consequent formation of a $C{=}CH_2$ function, which in turn causes a parallel increase in the adjacent $C{=}N_{imine}$ bond length [N(1)−C(2) = 1.380(9) Å, N(3)−C(8) = 1.375(9) Å].

The room-temperature magnetic moment of **4** in the solid state [μ_{eff} = 5.8 μ_B] compares well with the other complexes reported in this work and is in agreement with the metal divalent state. The connectivity of **4**, as yielded by the X-ray structure (Figure 4), clearly shows that the two former imine methyl groups have been deprotonated to produce two ene-amido functions (Scheme 2). There are precedents for this type of behavior in the chemistry of this ligand system with several metals including manganese,[3] vanadium,[11] lithium,[9] and lanthanides.[9] In the present case, the formation of **4** indicates the existence of an alternative reaction pathway.

We have previously reported that, in some cases and depending on the electronic configuration of the metal, the formation of mono-deprotonated or doubly deprotonated species similar to **4** leads to a curious dimerization reaction via radical coupling of two $C{=}CH_2$ moieties.[3,5,6] This coupling (Scheme 2) requires electrons to be provided to the ligand system, which can be obtained either from an external reducing agent (as in the case of lanthanides)[6] or at the expense of the $C{=}CH_2$ bond, in turn triggering a one-electron reduction of the metal center.[3,5] In our preparation of complexes **2** and **4**, we occasionally observed the formation of a small, yet significant, amount of dark crystals of a new dimeric species {[{[2,6-(*i*-Pr)$_2$C$_6$H$_5$]N−C═(CH$_2$)}(C$_5$H$_3$N){[2,6-(*i*-Pr)$_2$C$_6$H$_5$]N═C CH$_2$}]Fe(CH$_2$SiMe$_3$)}$_2$ (**5**) (Figure 4). Unfortunately, no further purification was possible due to the low yield and poor solubility of this species, regrettably preventing full characterization. Only in one case the quality of the crystals was just sufficient to allow a crystal structure determination.[31] Although the poor quality of the diffraction data did not allow a full anisotropic refinement, the connectivity and main features of this new compound were at least demonstrated. The complex is dinuclear with the same arrangement previously observed in Co,[5] Ln,[6] and Mn[3] chemistry. The salient features are the tetracoordination of the Fe atom, the dinuclear structure, and the nondeprotonation of the residual carbon group attached to the imine function [C−C = 1.49 Å]. Given the presence of the alkyl group attached to the Fe atom the oxidation state of the metal center can be regarded as monovalent, from the *formal* point of view. The fact that a monovalent Fe is generated at the expenses of the ligand system is in line with the behavior of the Co derivatives.[5]

Further attempts to clarify the genesis of complex **5**, and to make this species available in larger scale, were carried out with a number of experiments at both low and room temperature and by changing the sequence of addition of the reagents. In an attempt to follow synthetic pathways successful with other metals, even reduction was probed by treating **4** with either NaH or K(naphthalenide).[3,5,6] However, only intractable materials systematically resulted from those attempts. On the other hand, given that to form complex **5** only one of the two imine Me groups must undergo deprotonation, we have synthesized the monodeprotonated lithium salt of the ligand [{[2,6-(*i*-Pr)$_2$C$_6$H$_5$]N−C═(CH$_2$)}(C$_5$H$_3$N){[2,6-(*i*-Pr)$_2$C$_6$H$_5$]N═CCH$_2$}]Li.[7b] Low-temperature addition of this anion to $FeCl_2$, followed by addition of 2 equiv of RLi afforded, again, only intractable materials. However, the low-temperature treatment of $FeCl_2$ with RLi, where presumably a thermally labile FeR_2 species might be formed, followed by addition of the ligand monolithium salt gave a new complex [{2,6-[2,6-(*i*-Pr)$_2$PhN−C═(CH$_2$)]$_2$(C$_5$H$_3$N)}Fe(CH$_2$SiMe$_3$)][Li(THF)] (**6**) in acceptable yield (Scheme 3). The magnetic moment in the solid state of this new species [μ_{eff} = 5.6 μ_B] is in line with those of the other compounds reported in this work.

Presumably, the reaction proceeds via formation of an intermediate adduct of FeR_2 with the monodeprotonated ligand. The failure of this species to gives reductive dimerization toward **5**, and its transformation instead to complex **6** is interesting. It

(31) Crystal data for **5**: $C_{74}H_{106}Fe_2N_6Si_2$, M_W = 1247.42, monoclinic, $P2_1/c$, a = 17.41 Å, b = 12.07 Å, c = 18.33 Å, β = 111.1°, V = 3851.8 Å^3.

Scheme 3

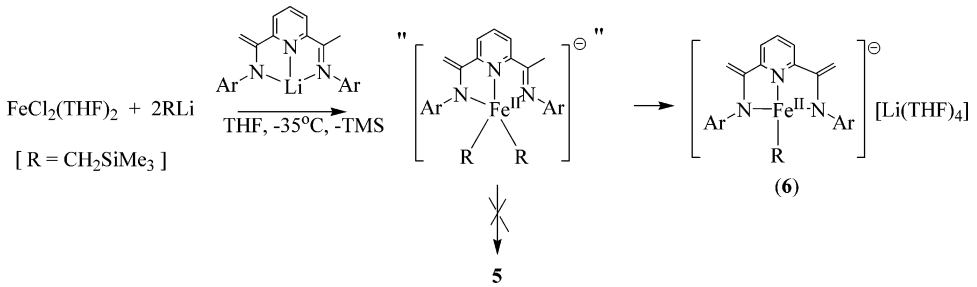

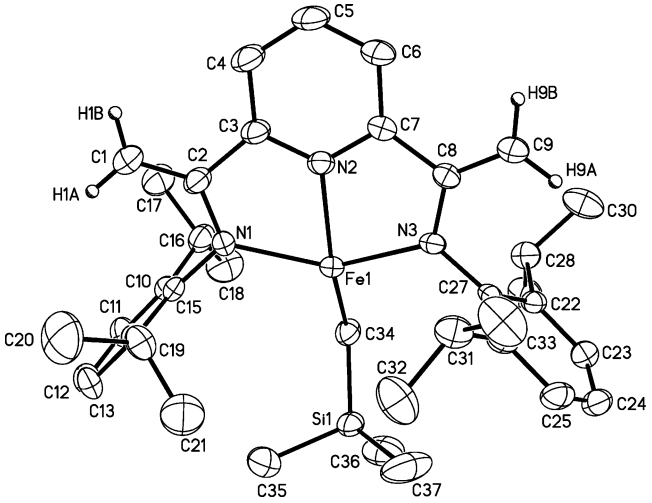

Figure 5. Thermal ellipsoid plot for **6** with the ellipsoids drawn at the 30% probability level. The THF-solvated cation has been removed for clarity.

suggests that a residual chlorine atom attached to Fe is important for the reductive dimerization and that the formation of the Fe−C bond in **5** occurs after the reduction of the metal center.

The crystal structure of **6** (Figure 5) is by all means comparable to **4** except for the lithium cation, which is solvated by four molecules of THF and unconnected to the Fe-containing anion. The bond distances and angles of the distorted square planar atom are very comparable [Fe(1)−N(1) = 2.094(4) Å, Fe(1)−N(2) = 2.138(4) Å, Fe(1)−N(3) = 2.078(4) Å]. The Fe−C distance [Fe(1)−C(34) = 2.068(5) Å] also compares well with those of **1**, **2**, **3**, and **5**. The coordination geometry around the Fe center displays a significant deviation from the planarity [C(34)−Fe(1)−N(2) = 155.41(18)°, N(1)−Fe(1)−N(3) = 145.67-(15)°, N(1)−Fe(1)−N(2) = 73.34(17)°]. The dianionic character of the ligand system is witnessed by the short C−C distances [C(1)−C(2) = 1.337(7) Å, C(8)−C(9) = 1.356(7) Å] formed by the C atom attached to the imine functions indicating a definite C−C double bond character. By the same token, the C−N distances are elongated [N(1)−C(2) = 1.360(6) Å, N(3)−C(8) = 1.354(6) Å].

There are interesting implications as far as the catalytic activity of these species is concerned. These complexes display high catalytic activity despite the tetracoordination (except **2**) and the high spin state at room temperature and atmospheric pressure and are very similar to that of the $FeCl_2$ adduct. Complexes **4** and **6** are twice as active comparably (Table 3). However, the polyethylene samples display very different natures. Complexes **1** and **2** form identical types of polyethylene showing a reasonably narrow distribution at low molecular weights and a minor amount of broadly dispersed PE at very high molecular weights (Figure 6, red line). In contrast, the formally monovalent **5** produces only broadly dispersed high molecular weight PE (Figure 6, blue line) while complex **4** shows an intermediate behavior in the sense that the two types of PE are present in comparable amounts in the sample (Figure 6, green line). As expected, complex **6** displays catalytic activity in the range of **4** and, more importantly, produces a similar polymer. This suggests that complexes **1** and **2** are related in the catalytic cycle and might lead to the same active species. However, the PE generated by **5** is also formed by **4** and **6**, therefore indicating that somehow, during the catalytic cycle, **4** and **6** gave reduction of the metal center. The reason for the remarkable difference between the samples of PE produced by complexes in the two different oxidation states is unclear. It may well be related to the different electronic configurations of the two oxidation states, which in turn relates to the relative stability of the intermediates involved in the chain propagation and termination steps.[32] At this stage, *it is interesting to observe that the monovalent species* **5** *is indeed catalytically very active* and that *all the species generated by the alkylation of the $FeCl_2$ adduct are catalytically active, altogether concurring to the polymerization process*.

Table 3. Polymerization Results

complex	temp (°C)	mass of catalyst (g)	MAO (equiv)	run time (min)	yield PE (g) (±0.10)	activity gPE/mmol cat/hr/atm
1	23	0.008	500	30	2.80	509
2	23	0.010	500	30	3.32	474
4	23	0.005	500	30	4.30	1433
5	23	0.007	500	30	3.60	654
6	23	0.006	500	30	3.30	1015
L-$FeCl_2$	23	0.007	500	30	3.90	678

DFT calculations on simplified models **1a**−**3a** (bearing just Me groups at Fe and the imine nitrogens; see Supporting Information) indicate that, for each of the Fe^{II} species considered, the IS (triplet, S = 1) and HS (quintet, S = 2) states are close in energy, with the LS (singlet, S = 0) state always being significantly higher (Table 4). These results agree with our experimental observation of a paramagnetic ground state for **1** and **2**. They might also be relevant to the nature of the active species in the Fe polymerization system. The spin state of the catalytically active species has been at the center of a theoretical debate. The active species in the catalytic cycle (generated by mixing $LFeCl_2$ with MAO) has commonly been assumed to be $LFeR^+$. Initial theoretical work by Ziegler et al. on this system[16a] indicated that the HS state was too high in energy to be accessible for $LFeR_2$ and $LFeR^+$ and would anyhow not be able

(32) Schmid, R.; Ziegler, T. *Organometallics* **2000**, *19*, 2756.

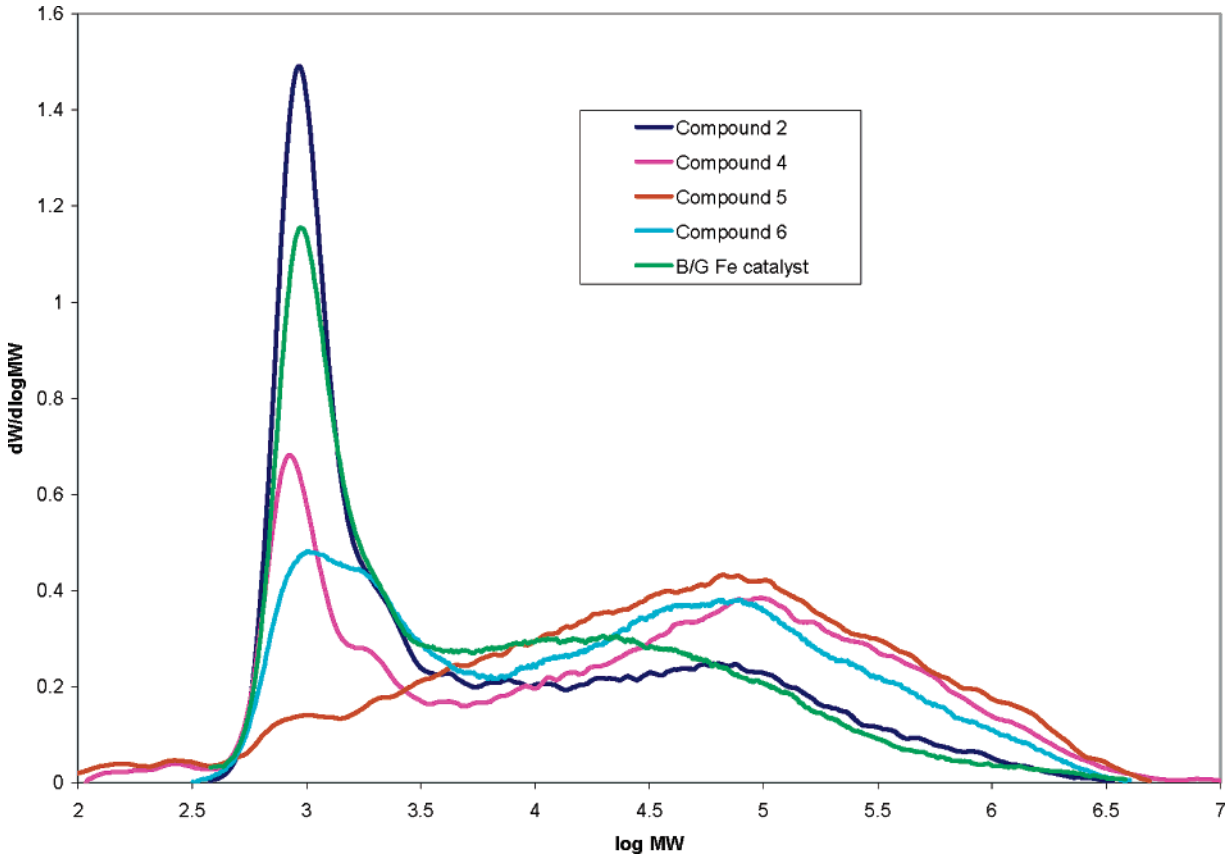

Figure 6. Gel permeation chromatogram of **1** and **2** (M_n 1860, M_w = 66 100, Ms 741 700, PD = 35.54), of **5** (M_n = 3250, M_w = 219 000, M_z = 1 207 000, PD = 67.38) of **4** (M_n = 2620, M_w = 207 300, M_z = 2 061 000, PD = 79.12), and of **6** (M_n = 3250, M_w = 219 000, M_z = 1 207 000, PD = 67.38).

Table 4. Calculated Relative Free Energies (kcal/mol) of L′FeMe$_2$ and Isomers in Different Spin States

complex	$S = 0$ (LS)	$S = 1$ (IS)	$S = 2$ (HS)	$S = 3$
L′FeCl$_2$	23.58	15.56	0.00	12.10
L′FeMe$_2$ (**2a**)	13.56	9.33	5.79	15.35
[2-Me−L′]FeMe (**1a**)	36.20	15.33	11.66	33.25
[*i*-Me−L′]FeMe (**3a**)	16.64	0.00	5.31	21.97
[N−Me−L′]FeMe[a]	37.15	16.28	10.48	43.24
L′FeMe$^+$	24.13	8.49	0.00	32.70

	$S = {}^1/_2$	$S = {}^3/_2$	$S = {}^5/_2$
L′FeMe	1.25	5.03	0.00

[a] Adduct with Me group at pyridine nitrogen.

to perform polymerization. Therefore, it was concluded that the LS state was probably involved in the polymerization, although participation of the IS state could not be excluded. The results of separate calculations by Morokuma[16c] and Zakharov[17] instead indicated that the LS state is highest in energy, while IS and HS states are close. Our calculations are more in line with these results. Given that our *experiments* indicate that LFeR$_2$ is already HS, and that our *calculations* indicate an even larger preference for the IS/HS states for LFeR$^+$ than for LFeR$_2$, we tentatively conclude that any LFeR$^+$ species involved in polymerization will *not* be low-spin. Of course, it remains possible that the catalytic cycle of this system does not involve LFeR$^+$ at all.[17] In the Fe^{II} complexes studied here, IS or HS states are preferred in which the diiminopyridine ligand appears to be electronically innocent; i.e., the complexes truly contain Fe^{II}. In contrast, for the formally monovalent L′FeMe **5a** (model for one-half of dimer **5**) the energies of $S = {}^1/_2$, ${}^3/_2$, and ${}^5/_2$ states are predicted to be all very close in energy (within a few kcal/mol). The $S = {}^1/_2$ state is best described as containing IS Fe^{II} antiferromagnetically coupled to a ligand radical anion, i.e., analogous to the situation in the diamagnetic formally Co^I alkyls LCoR.[33]

It is interesting to observe that the extent of simplification used for the calculation changes the relative order of stability of the complexes. According to the calculations on the simplified model systems, the IS state of imine adduct **3a** is the most stable of all species considered: it is lower than the corresponding HS state (by 6 kcal/mol) and all other isomers considered (by 4−17 kcal/mol). This disagrees with the experimental observations and indicates that steric effects play an important role here. Indeed, geometry optimization of the full systems **1**−**3** changes the order of stability completely. The estimated free energies of all HS states are now lower than those of the corresponding IS states (Table 5, last column). The dialkyl **2** is lowest in energy, followed by the two-adduct **1** at 4 kcal/mol and the imine adduct **3** at 6 kcal/mol. This revised stability order agrees well with experiment. However, it also indicates that if the bulky alkyls were to be exchanged for smaller Me or *n*-alkyl groups (as could happen during initiation with MAO), the Fe dialkyl might no longer be the most stable isomer, with the imine adduct becoming at least as favorable. In view of the remarkable ease of alkyl shift between the imine moiety and the metal atom observed in the present work, it seems that some form of ligand alkylation might well be important in activation of the Fe complex.

(33) Knijnenburg, Q.; Hetterscheid, D.; Kooistra, T. M.; Budzelaar, P. H. M. *Eur. J. Inorg. Chem.* **2004**, 1204.

Table 5. Effect of Steric Bulk on Alkyl Transfer Energetics (IS and HS States Only; kcal/mol)

system	ΔE_{model}	ΔG_{model}	ΔE_{full}	ΔG_{full} (est)[a]
$LFeR_2$ (**2**) IS	10.75	9.33	4.28	8.16
HS	12.10	5.79	1.42	0.00
[2-R−L]FeR (**1**) IS	16.94	15.33	14.10	17.81
HS	13.34	11.66	0.00	4.08
[*i*-R−L]FeR (**3**) IS	0.00	0.00	4.85	11.89
HS	6.79	5.31	0.17	6.16
[N−R−L]FeR IS	16.69	16.28	18.30	25.20
HS	11.07	10.48	5.13	12.35

[a] Obtained by combining the SV(P) energies for the full system with thermal and basis set (SV(P)→TZVPP) corrections for the model system.

Conclusions

In conclusion, with this study we have unveiled the remarkably complex behavior of the Gibson−Brookhart Fe catalyst in the presence of alkylating agents. The noninnocent behavior of this ligand system, as previously observed with several other transition metals and different alkylating agents, also dominates in the case of the Fe analogues. Different from the other cases, however, the mobility of the alkyl groups and the variety of transformations affect the redox chemistry only a little. The reduction of the metal center, which is a rather common feature in the case of other metals, seems to be confined exclusively to the dimerization pathway via coupling of two deprotonated imine C atoms or to a reaction carried out at room temperature. Otherwise, the combination of a divalent organo-iron species with this ligand system seems to be reasonably robust, once the complex is formed, at least with the particular alkyl used in this study. The fact that the monovalent species also displays very high catalytic activity and produces a distinctly different PE making it unlikely that a trivalent Fe species (possibly formed through disproportionative pathways) is involved in the catalytic cycle.

Acknowledgment. This work was supported by the Natural Science and Engineering Council of Canada (NSERC). We are indebted with NOVA (Calgary) for generous assistance with GPC measurements.

Supporting Information Available: Complete crystallographic data (CIF) for complexes **1**−**4** and complete ref 24c. This material is available free of charge via the Internet at http://pubs.acs.org.

JA054152B